Workflow for generating personalised anatomical models of the skeleton and the skin surface of the upper torso

Fangchao Pan[1], Kejia Khoo[1], Thiranja P. Babarenda Gamage[1], Gonzalo Maso Talou[1], Poul M.F. Nielsen[1,2], Martyn P. Nash[1,2]

Abstract Breast cancer is the leading cause of cancer-related death in women worldwide. Diagnostic imaging such as 3D magnetic resonance imaging (MRI) is acquired with patients positioned in the prone orientation with arms either above their heads or by their sides. However, treatment procedures such as surgery are performed in the supine position. Differences in the skeletal pose, and the large deformations that the breast undergoes during repositioning, make it challenging to localise breast lesions during treatment procedures. To address this issue, biomechanical modelling workflows have been proposed to simulate breast tissue deformation following patient repositioning. A key step in these workflows is the automated construction of personalised anatomical models to describe the geometry of the individual's breast tissues. Previous workflows have focused on modelling the soft tissue boundaries near the breast region without considering the individual's pose and skeletal joint positions. The proposed workflow uses a human body model as a template to obtain an initial estimate of each individual's shape before performing local refinement. The workflow is being designed to model data from multiple poses, and it incorporates skeletal information enabling more realistic boundary conditions to be applied during breast biomechanics simulations.

[1]Auckland Bioengineering Institute, University of Auckland, New Zealand

[2]Department of Engineering Science, University of Auckland, New Zealand

1 Introduction

Breast cancer is the leading cause of cancer-related death in females, affecting one in every ten women worldwide [1]. During treatment, the patient usually lies in a supine position, whereas the diagnostic image of the breast is typically acquired in a prone position. The relative change in gravity loading can cause significant deformation in the breast tissues, creating ambiguity for the surgeon in locating tumour positions. To address this issue, biomechanical models have been developed to simulate breast deformation due to gravity and changes in pose. One of the key steps for biomechanical simulation is to construct a personalised anatomical model that provides descriptions of the geometry of the breast tissues. Many studies have focused on creating personalised anatomical models to represent the soft tissue boundaries of the breast (e.g.,[2] – [6]). However, existing biomechanical models typically consider only the region surrounding the breasts without considering the individual's skeletal pose. The joint positions of the arms and shoulders need to be considered as they influence the shape and stretch level of the pectoral muscles upon which the breast sits. During the imaging process, the subject's arm and shoulder can be placed in a variety of positions, significantly altering the shape of the pectoral muscles, and impacting the position and deformation of the breast. Articulated human body models are used in the computer graphics field to generate realistic-looking 3D human body surfaces. These parameterised human body models were trained using large datasets to model the variation in body shapes and pose-related deformation on the skin surface. They are widely adopted for their robustness, controllability, flexibility, and efficiency. Some of the most successful human body models include SCAPE [7], SMPL [8], and STAR [9]. Numerous studies [10] [11] have been conducted to register such human body models to 3D scans of the entire human body. However, current human body models rely on very naive and anatomically unrealistic representations of the human skeleton, in contrast to anatomically accurate multi-body skeletal models that are widely adopted in the field of biomechanics analysis [12] – [14].

This manuscript aims to describe an automated workflow for the generation of personalised anatomical meshes of the torso that incorporates anatomically accurate models of the skeleton for biomechanics simulations. A multi-body model is developed and personalised using the OpenSim software [15] to model the relevant skeletal joints for each individual. We employ an articulated human body model as the template model to obtain an initial estimate for the skin surface. The initial estimate is then locally refined to capture more details on the skin surface. The workflow assimilates 3D medical data from multiple positions.

Incorporating skeletal modelling into the workflow enables personalised boundary conditions to be applied during breast biomechanics simulations. The constructed meshes also provide a basis for statistical shape analysis of the torso in multiple poses.

2 Methods

This section will describe the methods used to generate personalised anatomical surface meshes of the skeleton and the skin surface of upper torso. Subsection 2.1 will introduce the data used to test and evaluate the workflow. Subsections 2.2 and 2.3 will introduce the personalisation process of the skeleton and skin surface models, respectively.

2.1 Image Acquisition and Pre-processing

This workflow was tested and evaluated using MR images in a dataset acquired by the Biomechanics for Breast Image Group at The Auckland Bioengineering Institute (ABI). The full dataset consists of high resolution (1 mm^3) T1- and T2-weighted MR images that were acquired from 110 healthy participants in prone and supine positions at the University of Auckland's Centre for Advanced Magnetic Resonance Imaging (CAMRI). Landmarks on relevant skeletal joints were manually placed on the MR images (See Table 1 for a complete list of the identified landmarks and their definition). Meshlab software was used to generate triangulated surface meshes (hereinafter referred to as data meshes) from the manually segmented skin surface boundaries observed in the prone MR images.

Landmarks	Definition for manual identification
Sternal notch	The most superior, anterior point at the centreline of the manubrium
SC	The most anterior, superior point at the medial end of the clavicle
AC	The most posterior, lateral point on the acromion of the scapula
GH	Centre of the humeral head

Table 1. A list of manually identified landmarks in the MR image and their definition.

2.2 Skeletal Model Personalisation

A multi-body model of the torso developed in OpenSim [14] was used as the template model for the skeleton. The model has 23 degrees of freedom, parameterised on the sternum, sternoclavicular (SC), acromioclavicular (AS), glenohumeral (GH), humeroulnar and ulnoradial joints. The template model is in a standard anatomical position, which is defined as standing erect, looking forward, with the feet close and parallel to each other, the arms at the side and the palms facing forward [16].

Personalisation of the template model is achieved through scaling each component (e.g., each bone) of the model to match joint landmark positions identified in the MR images (See Table 1) for a given subject. The optimal scaling factor was computed using Scipy version 0.24 [17]. Specifically, the objective function quantifying the distance error between joint landmarks is defined as

$$\mathrm{F}(\boldsymbol{s}) = \frac{\sum_{p=1}^{P}\sum_{i=1}^{N}\left|\left|z_{i,p}(\boldsymbol{s})\right|\right|}{P} \quad (1)$$

where $\boldsymbol{s}$ is the vector of scaling parameters in each of the *x*, *y,* and *z* axes to be optimised, and $\left|\left|z_{i,p}(\boldsymbol{s})\right|\right|$ is the Euclidean distance between the corresponding i^{th} joint centre point on the template model and MRI data in the p^{th} body position, N is the number of joints and P is the number of body positions (e.g., prone or supine). Once the scale parameters were identified, the joint angles were subsequently determined using the inverse kinematic solver provided in the Python API of OpenSim 4.0 [15]. The objective function to minimise is the energy defined as

$$E_{\phi} = \left|\left|\boldsymbol{J}_{MRI} - \boldsymbol{J}_{\mathcal{O}}(\phi)\right|\right|_{F} \quad (2)$$

where ϕ are the joint angles in the template model with respect to the standard anatomical position, $\boldsymbol{J}_{\mathcal{O}}$ and $\boldsymbol{J}_{MRI}$ are matrices related with the joint positions in the template model and MRI data, respectively. Specifically, $\boldsymbol{J} = [\boldsymbol{j}_1^T, \ \ldots, \boldsymbol{j}_K^T]$, where the 3-element vector $\boldsymbol{j}_k$ represents the 3D coordinates of the k^{th} joint. In our workflow $K = 7$. The optimised joint angles describe the pose of the individual seen in the MRI (see Fig. 1).

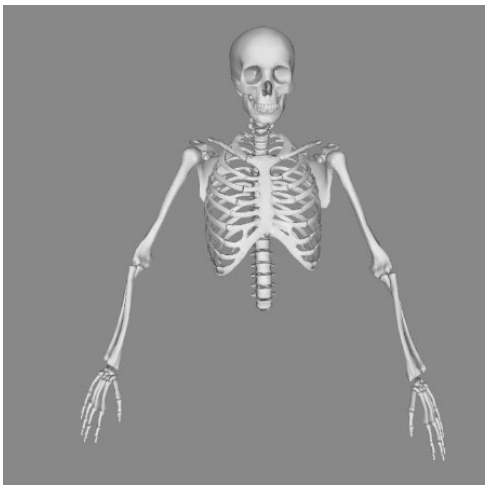

Fig. 1. The personalised multi-body skeleton model generated using the proposed workflow for a volunteer in the prone position.

2.3 Skin Surface Model Personalisation

To deal with the complex geometry of the human skin surface in multiple poses, an articulated human body model was used as a template model to generate an initial estimate of the geometry of the skin surface. The template model used in this workflow is a female version of the Skinned Multi-Person Linear model (SMPL) model [8]. SMPL is an articulated human body model that uses joint angles θ and body shapes descriptors β as input parameters and generates triangulated skin surface mesh of the human body based on population information (See Fig. 2a). The fitting process follows the concept of the Functional Automatic Registration Method (FARM) [11].

The personalised multi-body model estimated in the previous section is used to constrain key joint positions of the SMPL model. The template model was linearly scaled and aligned to match the position of shoulder joints in SMPL and those defined in the personalised skeleton model. We modified this model to only include vertices from the neck to the base of the thorax and upper sections of the arms. Note that the multi-body model has two joints to represent the kinematic movement of shoulders (glenohumeral and acromioclavicular), whereas SMPL uses only one joint. Thus, the midpoints of glenohumeral joints and acromioclavicular joints in the multi-body model were considered as the shoulder joint for optimisation.

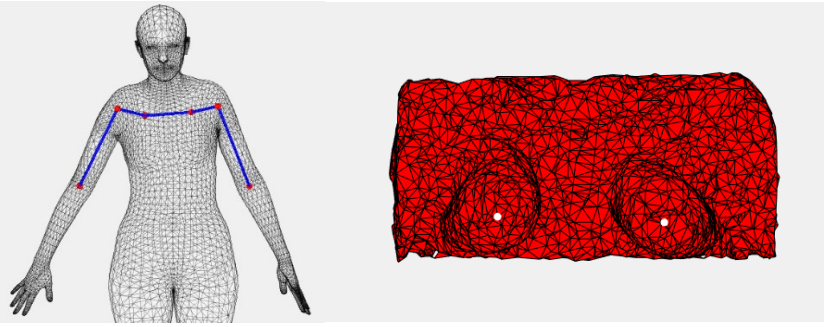

(a) (b)

Fig. 2. SMPL (a) is employed as the template model in this workflow, where red points are the estimated joint positions. (b) is the data mesh generated from segmented MR data using Meshlab software, where white dots are landmarks placed on the nipples.

The template model was non-rigidly registered to the data mesh generated from the manually segmented skin surface boundaries observed in the prone MR image (see Section 2.1), obtaining an initial estimate of the individual's shape. The registration process can be described as follows. To initialise the process, left and right nipple landmarks were placed on the data mesh (see Fig 2b) and template model. Specifically, the landmarks are placed on the most anterior point of each breast. Dense correspondences between the template model and the data mesh were computed using the functional map approach. The goal is to compute a point-wise map

$$\pi: \mathcal{N} \rightarrow \mathcal{M} \tag{3}$$

where operator π maps points on the data mesh domain $\mathcal{N}$ to the corresponding points on the template model domain $\mathcal{M}$ (See Fig 3a and b). Functional map approach uses real-valued functions defined on each shape, such as the eigenfunctions of its Laplace-Beltrami operator, to obtain a more compact representation of a map between two shapes. The original map π can be reconstructed from the functional representation. We refer the readers to the references [11] and [18] for the details. The map π will constrain the non-rigidly fit of the template model to the data mesh.

(a) (b)

Fig. 3 Dense correspondences between the (a) data mesh and (b) template model. Computed correspondences are displayed in the same colour.

The initial estimate of the skin surface is obtained by minimising the following energy:

$$\mathcal{E}(\beta,\theta) = w_V E_V(\beta,\theta) + w_L E_L(\beta,\theta) + w_\beta E_\beta(\beta) \quad (4)$$

with respect to the shape β and pose θ parameters in the SMPL model that instantiate the template model domain $\mathcal{M}$. Here, E_V is the term measuring the alignment error between surface vertices of the two shapes

$$E_V = \left|\left|\boldsymbol{X}_{\mathcal{M}} - \pi(\boldsymbol{X}_{\mathcal{N}})\right|\right|_F \quad (5)$$

where $\boldsymbol{X}_{\mathcal{M}}$ are the vertices on the template model, and $\pi(\boldsymbol{X}_{\mathcal{N}})$ are the corresponding points identified by the mapping π. Similarly, E_L represents the discrepancies between landmarks on the model and data

$$E_L = \left|\left|\boldsymbol{L}_{\mathcal{M}} - \boldsymbol{L}_{\mathcal{N}}\right|\right|_F \quad (6)$$

where $\boldsymbol{L}_{\mathcal{M}}$ and $\boldsymbol{L}_{\mathcal{N}}$ are the positions of landmarks placed on the model and data mesh, respectively. E_β is defined as

$$E_\beta = \left|\left|\beta\right|\right|^2 \quad (7)$$

which regularises the shape parameter. Regularisation weights, w, in the workflow are set to $w_V = 1$, $w_L = 1$, and $w_\beta = 0.05$.

Until this step, all optimisations are with respect with SMPL parameters β and θ. Since SMPL can only model human body shape within the span of its training set, the model is at our disposal, and further local refinement can be applied directly. In this workflow, an as-rigid-as-possible (ARAP) algorithm [19] is employed in conjunction with a nearest-neighbour energy to get the locally refined mesh.

3. Result and Discussion

Personalisation of the multi-body skeleton model was applied to MR images of 12 individuals in the dataset. To quantify the fitting accuracy, we define an error metric as the distance between the modelled joint positions and the landmarks placed in the MR images. Applying the multiple pose optimisation method results in a mean error of 2.4 mm ± 2.3 mm.

The main source of error is the uncertainty incurred in manual identification of landmarks in MR images. Repeatability in landmark identification was investigated by selecting the landmarks for each volunteer ten times. The order of landmarks was randomised and performed over two sessions. Standard deviation is used to measure the uncertainties of landmark placement. The uncertainties in the placement of landmarks are 2.3 mm, 1.9 mm, 2.6 mm, and 0.9 mm for the sternal notch, SC, AC, and GH joints, respectively. The uncertainties in the landmark placement process could lead to significant inaccuracies during the personalisation of the multi-body model. The accuracy of kinematic models depends on how well the underlying model matches the subject's anthropometric data. However, previous studies have shown that the linear scaling method has a higher error when compared to statistical shape modelling scaling [20].

Due to the lack of manually segmented data and poor visibility of key joint landmarks in the MR image, the personalisation of skin surface was applied to MR images of three individuals in the dataset. See Fig 4a and 4b for an example of the fitted mesh. Hausdorff distance the skin surface segmented from the MRI and the fitted skin surface was used to quantify the performance of the workflow. The mean Hausdorff distances for three individuals are 5.1 mm, 4.9 mm, and 7. 8mm. The mesh shows noticeable poor fits around the sternum region because the template model being employed in the workflow was trained using clothed people in upright positions. The workflow is also sensitive to data partiality, as missing parts may cause shape matching between the data and the template to fail.

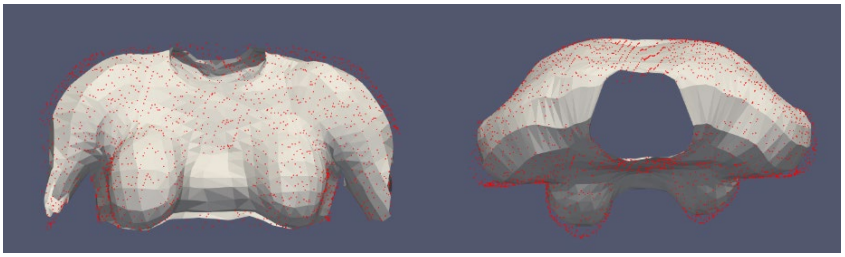

(a) (b)

Fig 4. Refined mesh from the (a) anterior view and (b) superior view, where points are the segmented point clouds from a MR image acquired in the prone position.

The proposed workflow for the skin surface is automatic and requires minimal manual intervention. The functional map algorithm matches correspondences on the

template model and the data without regarding the individual's body size, pose, and orientation. The template model patches small holes and fixes minor artefacts on the segmented data. This approach also uses population information on female body shapes, since SMPL is the first human body model that used the entire CAESAR [21] dataset for training. However, one of the key limitations of this workflow is that the training data of SMPL (as well as other human body models in the field) consists of scanned people who are wearing tight clothing and standing in an upright position. This makes the template model unable to capture anatomical details on bare breasts when the individual is in the prone position, leading to poor initial estimates and will subsequently destabilise the process of local refinement.

Although the approach is automatic, the correspondence matching algorithm employed in the workflow is vulnerable to any change of topology. A major limitation of this workflow is the partiality of data, where the data observed in the MR image is a subset of the template model. The inconsistency of the field of view causes difficulties in the model fitting process. For example, a template model with the neck included may not be suitable for those data without the neck region segmented since the correspondences on the neck region do not exist. Moreover, shoulder joints are only visible in less than 40% of the MR images in our dataset due to limited field of view. Extending the field of view would allow more skeletal joint to be identified, providing more constraints for skin surface mesh construction.

In the future, a mapping algorithm that specialises in matching partial shapes will be deployed. A partial map enables the alignment of whole-body models without considering the completeness of the input data. Furthermore, the robustness of this workflow will be quantitatively assessed by fitting it to a larger cohort. It should be remarked that the SMPL representation of joints does not accurately represent the anatomical structure of the human skeleton. A better mapping between the multi-body and human body models to align the template models is within the scope of future works. Alternatively, the 1D multi-body skeleton model can be replaced with a more representative statistical shape model, potentially providing a more accurate estimate of joint positions compared to the linear scaling of the multi-body model.

4. Conclusion

This study proposed a workflow to generate skin surface meshes of the female torso from medical imaging. In contrast to previous works which mainly focused on regions near the breast without regarding the skeletal pose, this workflow is being designed to account for multiple poses. Additionally, the workflow incorporates anatomically accurate models of the skeleton. The constructed skin surface meshes provide a basis for statistical shape analysis of the torso in multiple poses.

Acknowledgments The authors are grateful for financial support from the New Zealand Government Ministry for Business, Innovation and Employment (UOAX1004), the University of Auckland Foundation (F-IBE-BIP), and the New Zealand Breast Cancer Foundation (R1704).

References

1. Bray F, Ferlay J, Soerjomataram I, Siegel RL, Torre LA, Jemal A (2018) Global cancer statistics 2018: GLOBOCAN estimates of incidence and mortality worldwide for 36 cancers in 185 countries. *CA Cancer J Clin.* 68(6):394-424
2. Han L, Hipwell JH, Eiben B, et al (2013) A nonlinear biomechanical model based registration method for aligning prone and supine MR breast images. *IEEE Trans Med Imaging*. 33(3):682-694
3. Mîra A, Carton AK, Muller S, Payan Y (2018) A biomechanical breast model evaluated with respect to MRI data collected in three different positions. *Clin Biomech*. 60:191-199
4. Babarenda Gamage TP, Malcolm DTK, Maso Talou G, et al (2019) An automated computational biomechanics workflow for improving breast cancer diagnosis and treatment. *Interface Focus*. 9(4):20190034.
5. Eiben B, Han L, Hipwell J, et al (2013) Biomechanically guided prone-to-supine image registration of breast MRI using an estimated reference state. In: *2013 IEEE 10th International Symposium on Biomedical Imaging*. IEEE; 2013:214-217.
6. Han L, Hipwell JH, Tanner C, et al (2011) Development of patient-specific biomechanical models for predicting large breast deformation. *Phys Med Biol*. 57(2):455.
7. Anguelov D, Srinivasan P, Koller D, Thrun S, Rodgers J, Davis J (2005) SCAPE: shape completion and animation of people. In: *ACM SIGGRAPH Papers on - SIGGRAPH '05*. ACM Press; 2005:408.
8. Loper M, Mahmood N, Romero J, Pons-Moll G, Black MJ (2015) SMPL: a skinned multi-person linear model. *ACM Trans Graph*. 34(6):1-16.
9. Osman AAA, Bolkart T, Black MJ (2020) STAR: Sparse Trained Articulated Human Body Regressor. *ArXiv200808535 Cs*. 12351:598-613.
10. Zuffi S, Black MJ (2015) The stitched puppet: A graphical model of 3D human shape and pose. In: *2015 IEEE Conference on Computer Vision and Pattern Recognition (CVPR)*. IEEE; 2015:3537-3546.
11. Marin R, Melzi S, Rodolà E, Castellani U (2020) FARM: Functional Automatic Registration Method for 3D Human Bodies. *Comput Graph Forum*. 39(1):160-173.
12. Chadwick EK, Blana D, Kirsch RF, van den Bogert AJ (2014) Real-Time Simulation of Three-Dimensional Shoulder Girdle and Arm Dynamics. *IEEE Trans Biomed Eng*. 61(7):1947-1956.
13. Bruno AG, Bouxsein ML, Anderson DE (2015) Development and Validation of a Musculoskeletal Model of the Fully Articulated Thoracolumbar Spine and Rib Cage. *J Biomech Eng*.137(8):081003.
14. Kejia Khoo (2021) *Personalised Skeletal Modelling of the Female Torso from Multiple Loaded States*. M.S. Thesis. the University of Auckland.
15. Delp SL, Anderson FC, Arnold AS, et al (2007) OpenSim: Open-Source Software to Create and Analyze Dynamic Simulations of Movement. *IEEE Trans Biomed Eng*. 54(11):1940-1950.
16. Nikita E (2017). The Human Skeleton. In: *Osteoarchaeology*. Elsevier; 2017:1-75.
17 Virtanen P, et al (2020) SciPy 1.0: fundamental algorithms for scientific computing in Python," Nat. Methods, vol. 17.
18. Ovsjanikov M, Ben-Chen M, Solomon J, Butscher A, Guibas L (2012) Functional maps: a flexible representation of maps between shapes. *ACM Trans Graph*. 31(4):1-11.
19. Chao I, Pinkall U, Sanan P, Schröder P (2010) A simple geometric model for elastic deformations. *ACM Trans Graph TOG*. 29(4):1-6.
20. Bahl JS, Zhang J, Killen BA, et al (2019) Statistical shape modelling versus linear scaling: Effects on predictions of hip joint centre location and muscle moment arms in people with hip osteoarthritis. *J Biomech*. 85:164-172.

21. Robinette KM, Daanen H, Paquet E (1999) The CAESAR project: a 3-D surface anthropometry survey. In: *Second International Conference on 3-D Digital Imaging and Modeling (Cat. No. PR00062)*. IEEE; 1999:380-386.